JURNAL TEKNIK SIPIL CENDEKIA
e-ISSN : 2723-3375
doi : **10.51988/jtsc.v7i4.736**
pp : 778-786

Experimental Formulation of a Reynolds-Number- and Wall-Reaction- Based Correction Factor for Chlorine Transport in Pressurized PVC Pipes

Sumardi[1*], Farida Gaffar[2]
[1,2]Department of Water Resources Engineering, Faculty of Engineering, Universitas Muhammadiyah Makassar, Makassar, Indonesia
[*)]Correspondence writer (Sumardi@unismuh.ac.id)

Received : 8 September 2026 Revised : 13 Oktober 2026 Accepted : 28 Oktober 2026

Abstract

Accurate residual-chlorine prediction in pressurized water systems can be affected by the way one-dimensional models aggregate radial transport and pipe-wall processes. This study develops an empirical Reynolds-number-dependent correction for chlorine transport using controlled loop experiments. A 20 m PVC loop with a nominal diameter of 2 in was operated at eleven Reynolds numbers from 500 to 30,000. Each condition was tested in triplicate; chlorine was restored to 1.5 mg/L before each run and residual concentration was recorded hourly for 72 h. The analysis used a dimensionless wall-related term Z and a worksheet-defined percentage error E. For each Reynolds-number group, the normalized response was calculated as $\Phi = \bar{E}/\bar{Z}$ and fitted with a power law in logarithmic space. Parameter uncertainty and predictive performance were assessed using 95% confidence intervals, MAE, RMSE, MAPE, and leave-one-Reynolds-group-out cross-validation. Φ decreased from 0.300650 at Re = 500 to 0.003466 at Re = 30,000. The fitted relationship, $\Phi = 0.1306(Re/1000)^{-1.063}$, produced $R^2 = 0.9967$, RMSE = 0.0094, and MAPE = 5.69%; cross-validation yielded RMSE = 0.0140 and MAPE = 6.95%. The formulation is therefore proposed as a compact diagnostic correction within the tested PVC-loop range and should not be used as a substitute for system-specific hydraulic and water-quality calibration.

Keywords: *Reynolds Number, Correction Factor, Chlorine Transport, Wall Reaction, Pipe Network*

© Diterbitkan oleh Jurnal Teknik Sipil Cendekia 2026. This article is distributed under a Creative Commons Attribution-ShareAlike 4.0 International License.

INTRODUCTION

Maintaining a disinfectant residual throughout a distribution system is essential for microbiological protection, yet chlorine is continuously depleted by reactions in the bulk water and at pipe surfaces. Residual levels are also influenced by water age, temperature, source-water characteristics, pipe material, and hydraulic state. Field and modelling studies have shown that changes in operating conditions can materially alter residual profiles, reaction coefficients, and rechlorination or dosing requirements [1], [2], [5], [10], [11], [14], [16]. Accordingly, a model calibrated under one hydraulic regime cannot automatically be assumed to retain the same predictive accuracy when flow conditions change.

Network-scale water-quality models commonly use one-dimensional transport equations because they are computationally efficient and can be coupled directly with hydraulic solvers. This simplification is

practical, but radial concentration gradients and mass transfer toward the pipe wall are represented through aggregated terms. Earlier studies established the importance of pipe-wall chlorine loss [7] and showed that formulations combining axial convection with radial diffusion can better describe in-pipe decay under some conditions [17], [20]. More recent experiments have also reported Reynolds-dependent diffusion and dispersion behavior across laminar and transitional flow ranges [18]. These findings provide a mechanistic basis for expecting model discrepancy to vary with hydraulic regime.

Recent chlorine-transport research has expanded beyond conventional kinetic calibration. Artificial neural networks, recurrent models, sensor-assisted forecasting, and related data-driven approaches have been used to represent nonlinear decay and temporal variability in distribution systems [3], [4], [8], [9], [15], [19], [21]. At the same time, physically based studies continue to show that wall-reaction coefficients depend on pipe and operating conditions rather than behaving as universal constants [6], [12], [13]. Although advanced models can improve predictive capability, a compact relationship with explicit hydraulic meaning remains useful when the objective is diagnostic adjustment rather than full system emulation.

The present work examines response data obtained from a controlled PVC pipe loop operated over Re = 500–30,000. For each Reynolds-number group, the analytical worksheet contains a dimensionless wall-related quantity Z, a percentage-error response E, and an aggregated normalized correction response Φ. Initial inspection showed that Φ declines sharply as Re increases. The unresolved question is whether this trend can be represented by a statistically stable and physically interpretable equation across the tested range, and whether the fitted relationship remains robust when individual Reynolds-number groups are excluded from calibration.

This study therefore has four objectives: (1) to quantify how the worksheet-defined error varies with the wall-related parameter under different Reynolds-number conditions; (2) to formulate an experimentally supported power-law relationship between the normalized correction response and Reynolds number; (3) to evaluate predictive performance using goodness-of-fit statistics and leave-one-Reynolds-group-out cross-validation; and (4) to interpret the observed trend in relation to hydraulic regime and mass-transfer behavior. The principal contribution is the conversion of repeated 72 h loop tests spanning a broad Reynolds-number range into a compact, flow-sensitive correction relationship while clearly distinguishing measured evidence from mechanistic interpretation.

METHOD

Experimental Setup and Test Protocol

Experiments were performed in a closed-loop apparatus containing 20 m of PVC pipe with a nominal diameter of 2 in. Before each run, the test water was prepared at an initial chlorine concentration of 1.5 mg/L. The target Reynolds number was established by adjusting the flow-control valve until the desired hydraulic condition stabilized. The valve position was then kept unchanged throughout the corresponding test. All measurements were conducted at ambient laboratory temperature.

Eleven Reynolds-number conditions were examined: 500, 1,000, 1,500, 2,000, 3,500, 5,000, 7,500, 10,000, 15,000, 20,000, and 30,000. Residual chlorine was measured every 1 h for 72 h at each condition, and each test was repeated three times. Before every replicate, the chlorine concentration was restored to 1.5 mg/L so that all replicates began from the same nominal initial concentration. This design provides repeated laboratory observations under fixed pipe geometry and controlled hydraulic conditions.

For each test series, the flow-control valve was adjusted to the prescribed Reynolds-number condition before hourly chlorine measurements began. The same hydraulic setting was maintained throughout the 72 h observation period. After completion of one replicate, the loop was re-prepared and the initial chlorine concentration was restored before the next replicate. Testing then proceeded to the next Reynolds-number condition after three replicates had been completed.

Residual Chlorine Measurement Procedure and Replication

Residual chlorine was measured with a digital chlorine meter after the chlorine measurement mode or parameter had been selected on the instrument. Measurements were recorded at 1 h intervals for 72 h. Replicate-specific hourly measurements constituted the experimental basis of the analytical worksheet; however, the regression dataset available for this manuscript retains group-level and parameter-sweep response metrics rather than replicate-specific uncertainty estimates. Consequently, the primary power-law regression treats each Reynolds-number group as one aggregated unit, while replicate-to-replicate variability is acknowledged as a source of uncertainty that should be propagated in future analyses when the raw hourly series are available.

Experimental Configuration Summary

The test configuration comprised a 20 m PVC closed loop with a nominal diameter of 2 in, an initial chlorine concentration of 1.5 mg/L, a digital chlorine meter, ambient room temperature, eleven Reynolds-number conditions from 500 to 30,000, hourly sampling over 72 h, and three replicates per Reynolds-number condition. Flow was controlled by valve opening, and the initial chlorine concentration was restored to 1.5 mg/L before each replicate.

Hydraulic Parameters and Data Reduction

Reynolds number was used to characterize the flow regime and was calculated in the conventional form:

$$Re = \frac{UD}{v} \quad (1)$$

where U is the mean flow velocity, D is the pipe diameter, and ν is the kinematic viscosity of water. The experiments used a fixed pipe configuration, while the target Reynolds number was achieved by adjusting discharge. Because the available experimental record specifies a nominal 2 in pipe diameter and ambient room temperature rather than a measured internal diameter and exact temperature series, those quantities were not used to introduce additional derived discharge or velocity values in this manuscript.

$$Z = \frac{2W_d L}{v} \quad (2)$$

The quantity Z was treated as a dimensionless parameter, as presented in the dataset. The correction factor used in the regression analysis was normalized as:

$$\Phi_g = E_g / Z_g \quad (3)$$

For each Reynolds-number condition g, the normalized response $\Phi_g$was derived from the relationship between the mean percentage error $\bar{E}_g$and the corresponding mean dimensionless wall-reaction parameter $\bar{Z}_g$. The values of $\bar{E}_g$and $\bar{Z}_g$were first obtained by averaging the respective quantities calculated from the experimental observations within each Reynolds-number condition. The normalized response was then defined according to Equation (3) as the ratio of these two mean quantities. This formulation provides a dimensionless measure of the relative discrepancy associated with wall-sensitive chlorine transport while allowing direct comparison across different flow regimes.

In addition to the group-level formulation, the ratio $E/Z$was evaluated for individual experimental observations to characterize the variation of the normalized response within each Reynolds-number condition. This step was used as a diagnostic analysis to determine whether the group-averaged response adequately represented the underlying variation across the range of wall-reaction parameters investigated. Thus, $\Phi_g$was not treated as an independently assigned parameter, but rather as a derived quantity obtained systematically from the experimentally determined error and dimensionless wall-reaction terms.

The resulting $\Phi_g$values were subsequently used to establish the functional relationship between the normalized correction response and Reynolds number. By expressing the correction response in this normalized form, the influence of flow regime could be examined independently of the absolute magnitude of the wall-reaction parameter, thereby providing the basis for deriving the Reynolds-number-dependent power-law formulation proposed in this study.

Power-Law Regression, Goodness of Fit, and Cross-Validation

The relationship between Φ and Reynolds number was represented by a power law because the aggregated points were

approximately linear on a log–log scale. The model was written as:

$$\Phi = a \left(\frac{Re}{100}\right)^{b} \quad (4)$$

Coefficients a and b were estimated by ordinary least squares after logarithmic transformation, $\ln(\Phi) = \ln(a) + b \ln(Re/1000)$. Parameter uncertainty was summarized using 95% confidence intervals based on t-distribution. Model performance was evaluated using R^2 in log space, mean absolute error (MAE), root mean square error (RMSE), and mean absolute percentage error (MAPE). To assess sensitivity to the small number of aggregated Reynolds groups, leave-one-Reynolds-group-out cross-validation (LOOCV) was also performed: the power law was refitted ten times for each withheld group, and the omitted Φ value was predicted from the remaining groups. Cross-validated RMSE, MAPE, and log-space R^2 were then calculated from the eleven withheld predictions.

The comparison series attributed in the source worksheet to Ozdemir and Ger (1998) was fitted using the same power-law procedure. This comparison is used only to evaluate how the two empirical relationships represent the present aggregated dataset; it is not intended as a reconstruction of the full experimental conditions of the 1998 study. Relative differences were calculated for each Reynolds number to identify the hydraulic range over which the two relationships diverged most strongly.

Analysis Procedure

The analysis began with a systematic inspection of the data structure and identification of the eleven Reynolds-number groups. For each group, the parameter-sweep pairs of Z and worksheet-defined error E were extracted, together with the group-level normalized response Φ and the reference-series value. This step preserved the full range of Z represented within each Reynolds group while keeping the eleven aggregated Φ values as the units used for the power-law regression.

The error–Z relationship was first examined at representative Reynolds numbers to determine how model discrepancy changed across the wall-related parameter sweep. The row-level E/Z distributions were then compared among Reynolds groups as an additional diagnostic of robustness. The aggregated Φ values were subsequently fitted with the power-law model in logarithmic space, with 95% confidence intervals estimated for the regression parameters.

Model performance was quantified using MAE, RMSE, MAPE, log-space R^2, relative deviation from the reference series, and LOOCV prediction error. The statistical patterns were finally interpreted in terms of flow regime, residence-time implications, radial mass-transfer sensitivity, and wall-related effects, while avoiding claims that were not directly measured by the experiment.

RESULTS AND DISCUSSION

Response of Numerical Error to the Wall-Reaction Parameter

Within each Reynolds-number group, the numrical error increased with Z, although the rate of increase varied strongly with flow regime (Figure 1). Curves at low Reynolds numbers were markedly steeper than those at high Reynolds numbers. Thus, for a comparable increase in the wall-related parameter, the calculated discrepancy was more sensitive under weaker-flow conditions.

This pattern is consistent with the expected hydraulic consequences of low flow. In a fixed loop, lower mean velocity increases characteristic residence time and reduces the relative dominance of axial convection, allowing radial gradients and wall-directed transport to contribute more strongly to concentration evolution. The experiment did not directly measure radial concentration profiles; therefore, the observed behavior is interpreted as being consistent with increased radial mass-transfer sensitivity rather than as direct proof of radial-diffusion dominance. This interpretation agrees with the two-dimensional framework of Ozdemir and Ger (1998), the Reynolds-dependent diffusion/dispersion measurements of Ozdemir et al. (2021), and recent evidence that chlorine-wall reactions should be linked to pipe-specific and hydraulic conditions [6]; [12].

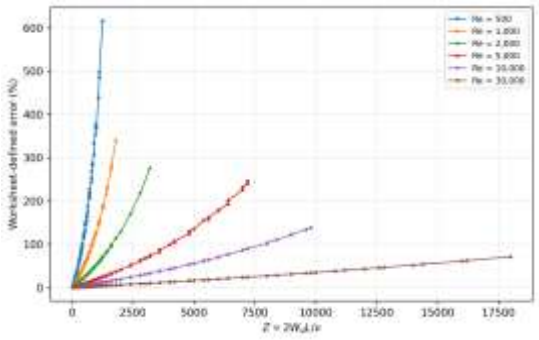

Figure 1. Numerical error as a function of Z for representative Reynolds numbers

Reynolds-Number-Based Correction-Factor Formulation

The aggregated normalized response Φ decreased monotonically from 0.300650 at Re = 500 to 0.003466 at Re = 30,000, corresponding to an overall reduction of approximately 98.85%. On a log–log scale, the relationship was close to linear, indicating that a single power law provides a compact representation across the tested Reynolds-number range.

$$\frac{100F_C}{Z} = 0.1306\left(\frac{Re}{1000}\right)^{-1.063} \quad (5)$$

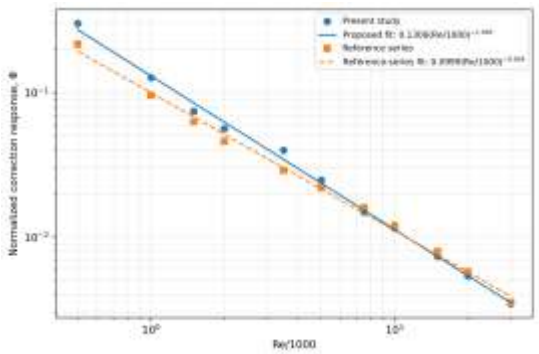

Figure 2. Power-law relationship between Φ and Re/1000, compared with the reference series identified in the source as Ozdemir and Ger (1998)

Equation (5) produced a log-space R^2 of 0.9967. The coefficient a had a 95% confidence interval of 0.1193–0.1430, while the exponent b ranged from −1.109 to −1.017. Because b is close to −1, the normalized correction response exhibits an approximately inverse dependence on Reynolds number. The response is therefore steepest in the low-Reynolds region and becomes progressively less sensitive as the flow strengthens.

Table 1. Summary of correction factor at each Reynolds number

Re	Φ (Present study)	Reference series	Relative difference (%)
500	0.300650	0.21700	38.5
1000	0.126872	0.09600	32.2
1500	0.074289	0.06300	17.9
2000	0.056315	0.04600	22.4
3500	0.039925	0.02900	37.7
5000	0.024852	0.02200	13.0
7500	0.014897	0.01600	-6.9
10000	0.011511	0.01200	-4.1
15000	0.007338	0.00795	-7.7
20000	0.005398	0.00578	-6.6
30000	0.003466	0.00355	-2.4

Goodness-of-Fit, Reference Comparison, and Cross-Validation

The aggregated Φ values closely followed the proposed prediction line across the tested Reynolds-number range (Figure 3). Against the present aggregated data, Equation (5) yielded MAE = 0.0051, RMSE = 0.0094, and MAPE = 5.69%. The fitted reference relationship yielded RMSE = 0.0335 and MAPE = 12.59% against the same data. The proposed relationship therefore reduced RMSE by approximately 72% and MAPE by approximately 55% relative to the fitted reference series.

The improvement was concentrated mainly at low Reynolds numbers. At Re = 500, Φ was approximately 38.5% higher than the reference series, and positive differences remained evident through Re = 5,000. The sign changed near Re = 7,500, after which the two relationships converged to within a few percent at medium-to-high Reynolds numbers (Figure 4). This behavior reflects the different slopes of the two power laws: −1.063 for the present dataset and approximately −0.954 for the fitted reference series.

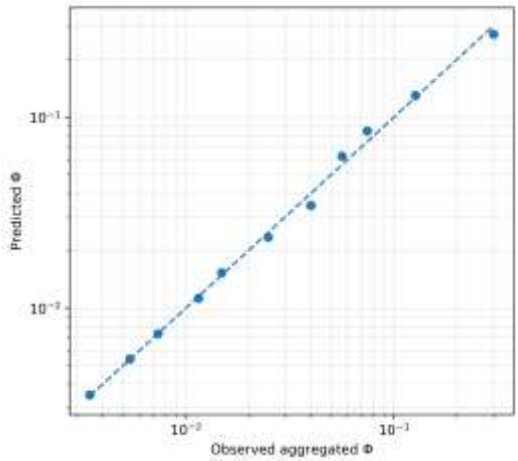

Figure 3. Agreement between aggregated Φ values and predictions from the proposed power-law equation

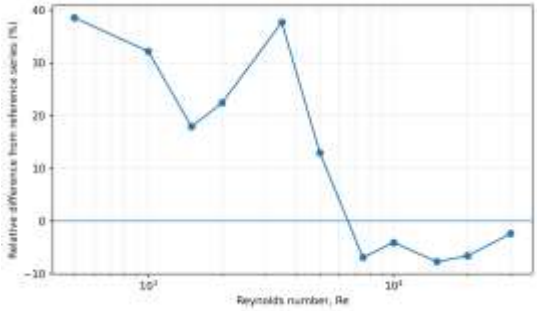

Figure 4. Relative difference between from the present study and the reference series at each Reynolds number

Table 2. Parameters and goodness-of-fit statistics for the power-law relationships

Parameter/metric	Proposed equation	Reference-series fit
Coefficient a	0.1306	0.0999
Exponent b	-1.063	-0.954
R^2(log space)	0.9967	0.9961
RMSE against present data	0.0094	0.0335
MAPE against present data	5.69%	12.59%

Distributional Robustness Across the Parameter Sweep

The aggregate power-law trend was also supported by the row-level parameter-sweep data. Figure 5 shows the distribution of E/Z within each Reynolds-number group. The entire distribution shifts downward as Reynolds number increases: the median E/Z decreases from approximately 0.226 at Re = 500 to 0.00333 at Re = 30,000, while the interquartile range also narrows. This pattern indicates that the Reynolds dependence is not produced solely by the eleven group means; it is visible across the broader set of Z conditions retained in the analytical worksheet.

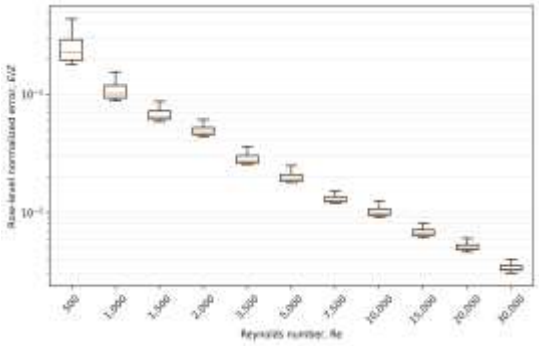

Figure 5. Distribution of row-level normalized error E/Z across Reynolds-number groups

Leave-one-Reynolds-group-out cross-validation provided an additional check against overfitting the eleven aggregated points. The withheld-group predictions produced RMSE = 0.0140, MAPE = 6.95%, and log-space R^2 = 0.9950. The largest relative deviations occurred in the low-to-transitional range, while predictions at Re ≥ 5,000 were generally close to the observed aggregate values (Figure 6). The cross-validation errors therefore remain modest relative to the approximately two-order-of-magnitude decline in Φ across the full Reynolds range, although the pattern also suggests that future datasets could test whether a piecewise formulation improves local accuracy in the low-to-transitional regime.

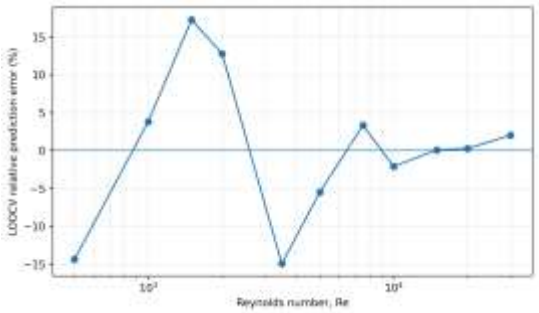

Figure 6. Relative LOOCV prediction error for each withheld Reynolds-number group

Hydraulic Interpretation and Relevance to Chlorine-Transport Modeling

The principal value of Equation (5) lies not only in its high coefficient of determination but in the shape of its response. The largest correction occurs at low Reynolds numbers, which correspond to weaker advection and longer characteristic residence times in a fixed pipe loop. Under these conditions, radial concentration gradients and wall-directed mass-transfer processes have more time to influence the overall concentration response. As Reynolds number increases, the normalized correction declines sharply and the difference from the reference series becomes progressively smaller.

These findings are consistent with recent chlorine-transport research emphasizing the combined roles of wall reaction, hydraulic state, temperature, and pipe material [6]; [12]; [13]. Data-driven approaches can further improve prediction by exploiting sensor data and operational histories [9]; [21]; [4]. The present relationship is not intended to replace such models. Its advantage is diagnostic transparency: the direction and magnitude of the normalized correction can be traced directly to Reynolds number and the wall-related parameter used in the analytical worksheet.

For network applications, Equation (5) should therefore be used as a correction or diagnostic layer only after the hydraulic state and water-quality reaction parameters have been established. Its use should be restricted to Re = 500–30,000, the range tested here. Full-scale residual-chlorine prediction still requires system-specific information on water age, bulk decay, wall reaction, temperature, pipe material, source-water quality, and hydraulic-model accuracy [1]; [11].

CONCLUSION

Laboratory-derived analytical data showed that the normalized correction response decreased systematically as Reynolds number increased. The relationship was represented by $\Phi = 0.1306(Re/1000)^{-1.063}$, with a log-space R^2 of 0.9967 and a 95% confidence interval of −1.109 to −1.017 for the exponent. Against the eleven aggregated Reynolds-group values, the proposed relationship yielded RMSE = 0.0094 and MAPE = 5.69%, whereas the fitted reference series yielded RMSE = 0.0335 and MAPE = 12.59%. Leave-one-group-out cross-validation produced RMSE = 0.0140 and MAPE = 6.95%, indicating that the fitted relationship remained stable when individual Reynolds groups were withheld.

The largest divergence from the reference relationship occurred at low Reynolds numbers, while the two relationships converged progressively as Reynolds number increased. The row-level E/Z distributions showed the same downward shift across the parameter sweep, supporting the robustness of the aggregated trend. Within the tested conditions—a 20 m PVC loop, nominal 2 in diameter, initial chlorine concentration of 1.5 mg/L, hourly measurements over 72 h, and three replicates per Reynolds condition—the equation can be used as a compact, physically interpretable diagnostic correction over Re = 500–30,000. It should not be treated as a substitute for hydraulic calibration, water-quality reaction calibration, or independent validation in a full-scale distribution system.

REFERENCES

[1]. Absalan, F., Hatam, F., Barbeau, B., Prévost, M., & Bichai, F. (2022). Predicting chlorine and trihalomethanes in a full-scale water distribution system under changing operating conditions. Water, 14(22), 3685. https://doi.org/10.3390/w14223685

[2]. Angassa, K., Feyisa, M., Tessema, I., & Abewaa, M. (2025). Residual chlorine modelling in drinking water distribution system of Bishoftu Town, Ethiopia. Results in Engineering, 25, 104075. https://doi.org/10.1016/j.rineng.2025.104075

[3]. Batista, G. S., de Lacerda, M. C., Aragão, D. P., de Araújo, M. M. C., & Rodrigues, A. C. L. (2024). Modeling the decay of free residual chlorine in water distribution networks in Brazilian rural communities using artificial neural network. Journal of Water Process Engineering, 61, 105312. https://doi.org/10.1016/j.jwpe.2024.105312

[4]. Brazil, G. R. M., Arai, Y., Iwamoto, T., Caronge, M. A., Kunizane, T., & Koizumi,

A. (2025). Long duration forecasting and its performance capability for seasonal variation modelling of residual chlorine concentrations: A comparative evaluation of two small-scale water distribution systems in Japan. Water Research, 268, 122766. https://doi.org/10.1016/j.watres.2024.122766

[5]. Costa, J., Mesquita, E., Ferreira, F., Figueiredo, D., Rosa, M. J., & Viegas, R. M. C. (2023). Modeling chlorine decay in reclaimed water distribution systems—A Lisbon area case study. Sustainability, 15(23), 16211. https://doi.org/10.3390/su152316211

[6]. Fisher, I., Kastl, G., & Sathasivan, A. (2023). Validity of chlorine-wall reaction models for drinking water distribution systems. Urban Water Journal, 20(9), 1157–1168. https://doi.org/10.1080/1573062X.2023.2241437

[7]. Hallam, N. B., West, J. R., Forster, C. F., Powell, J. C., & Spencer, I. (2002). The decay of chlorine associated with the pipe wall in water distribution systems. Water Research, 36(14), 3479–3488. https://doi.org/10.1016/S0043-1354(02)00056-8

[8]. Jafari, I., Luo, R., Lim, F. Y., Ng, S. H., & Hu, J. (2023). Machine-learning-assisted prediction and optimized kinetic modelling of residual chlorine decay for enhanced water quality management. Chemosphere, 341, 140011. https://doi.org/10.1016/j.chemosphere.2023.140011

[9]. Jafari, I., Luo, R., Ng, E., Corral, F., Jr., Chua, Y., Ng, S. H., & Hu, J. (2024). Robust prediction of residual chlorine decay in a drinking water distribution system integrating water quality sensing and predictive tools. ACS ES&T Water, 4(12), 5506–5521. https://doi.org/10.1021/acsestwater.4c00586

[10]. Jeong, G., Kang, D., & Hwang, T. (2022). Reaction coefficient assessment and rechlorination optimization for chlorine residual equalization in water distribution networks. Journal of Korea Water Resources Association, 55(S-1), 1197–1210. https://doi.org/10.3741/JKWRA.2022.55.S-1.1197

[11]. Kwio-Tamale, J. C., & Onyutha, C. (2024). Influence of physical and water quality parameters on residual chlorine decay in water distribution network. Heliyon, 10(10), e30892. https://doi.org/10.1016/j.heliyon.2024.e30892

[12]. Maleki, M., Pelletier, G., & Rodriguez, M. (2023). Identifying key pipe attributes and locations to best determine chlorine decay coefficients within a water distribution system. Water Supply, 23(10), 4333–4345. https://doi.org/10.2166/ws.2023.251

[13]. Maphanga, D., Moropeng, M. L., Masindi, V., Akinwekomi, V., & Foteinis, S. (2024). Experimental appraisal and numerical modelling of chlorine demand and decay in a typical drinking water distribution network in South Africa. Ecotoxicology and Environmental Safety, 286, 117153. https://doi.org/10.1016/j.ecoenv.2024.117153

[14]. Moeini, M., & Abokifa, A. (2024). Chlorine dosage management in drinking water systems: Comparing Bayesian optimization to evolutionary algorithms. Journal of Hydroinformatics, 26(11), 2720–2738. https://doi.org/10.2166/hydro.2024.090

[15]. Obaid, S., Hosoi, K., Ngoc, N. M., Inoue, T., & Yokota, K. (2025). Modelling free residual chlorine decay in a residential district water distribution network using smart water meter data. International Journal of Environmental Science and Technology, 22, 11809–11816. https://doi.org/10.1007/s13762-025-06378-5

[16]. Onyutha, C., & Kwio-Tamale, J. C. (2022). Modelling chlorine residuals in drinking water: A review. International Journal of Environmental Science and Technology, 19(11), 11613–11630. https://doi.org/10.1007/s13762-022-03924-3

[17]. Ozdemir, O. N., & Ger, A. M. (1998). Realistic numerical simulation of chlorine decay in pipes. Water Research, 32(11), 3307–3312. https://doi.org/10.1016/S0043-1354(98)00107-9

[18]. Ozdemir, O. N., Buyruk, T., & Ucaner, E. (2021). Calculation of chlorine and fluoride diffusion/dispersion coefficients in water supply pipes. Journal of Water Resources Planning and Management, 147(7), 04021041. https://doi.org/10.1061/(ASCE)WR.1943-5452.0001396

[19]. Riyadh, A., Zayat, A., Chaaban, A., & Peleato, N. M. (2024). Improving chlorine residual predictions in water distribution systems using recurrent neural networks. Environmental Science: Water Research & Technology, 10, 2533–2545. https://doi.org/10.1039/D4EW00329B

[20]. Ucak, A., & Ozdemir, O. N. (2002). Simulation of chlorine decay in drinking-water distribution systems. Journal of Environmental Engineering, 128(1), 31–39. https://doi.org/10.1061/(ASCE)0733-9372(2002)128:1(31)

[21]. Wei, S., Richard, R., Hogue, D., Mondal, I., Xu, T., Boyer, T. H., & Hamilton, K. A. (2024). High resolution data visualization and machine learning prediction of free chlorine residual in a green building water system. Water Research X, 24, 100244. https://doi.org/10.1016/j.wroa.2024.100244